INSERT CHAPTER NUMBER

THE LAGRANGIAN COORDINATES AND WHAT IT MEANS FOR FIRST ORDER TRAFFIC FLOW MODELS

Ludovic Leclercq, Jorge Laval and Estelle Chevallier, Laboratoire d'Ingénierie Circulation Transport (ENTPE/INRETS), Vaulx-en-Velin, France.

1. INTRODUCTION

Traditionally, first order traffic flow models have been formulated in Eulerian coordinates (x,t) as a scalar conservation law, namely the LWR model of Lighthill, Whitham (1955) and Richards (1956):

$$\partial_t k + \partial_x \left(kv \right) = 0 \tag{1}$$

This model is fully described by vehicle density k. The speed v and the flow q can be derived from a fundamental diagram (FD) $v=V(k)$ or $q=Q(k)=kV(k)$. This model is appealing because of its simplicity, parsimony and its robustness to replicate basic traffic features. Its solution is usually computed with the Godunov scheme (Godunov, 1959), which is based on iterative solutions of Riemann problems (Daganzo, 1994, Lebacque, 1996). Unfortunately, this scheme is known to introduce important numerical viscosity.

Alternatively, Newell (1993) proposed the use of the cumulative count function $N(x,t)$ and conjectured that the LWR solution is the lower envelope of the multiple values of $N(x,t)$ obtained from proper boundary and initial data. Recently, Daganzo (2005) proved Newell's conjecture using variational theory, which reduces the LWR model to the solution of the Hamilton-Jacobi equation:

$$\partial_t N = Q\left(-\partial_x N \right) \tag{2}$$

derived from $q=Q(k)$ since $k=-\partial_x N$ and $q=\partial_t N$. This new approach opened the door to powerful numerical methods based on shortest-path algorithms in (x,t) coordinates (Daganzo,2005b).

The aim of this paper is to go further into the use of the N-function by formulating the LWR model in the transformed coordinate system (N,t). These Lagrangian coordinates are fixed to a

given fluid particle and move with it in space-time. In this new coordinate system, the purpose is no longer to determine the local density k but the position $X(n,t)$ of vehicle number n. Note that in the continuum, n is not necessarily an integer. In the remainder of the paper, capital N (respectively X) will stand for the $N(x,t)$ (respectively $X(n,t)$) function while n (respectively x) will define a value taken by this function.
This paper is organized as follow: section 2 formulates the LWR model in Lagrangian coordinates as a conservation law and as a variational principle; it also derives relevant numerical schemes. Section 3 analyses the errors introduced by the Godunov scheme in Eulerian coordinates in order to gain some insights about its nature. Section 4 shows how to implement existing and novel extensions using the Lagrangian approach. Finally, section 5 presents a discussion.

2. THE LWR MODEL IN LAGRANGIAN COORDINATES

This section presents the continuum formulation of the LWR model in Lagrangian coordinates, as a conservation law and as a variational principle. Numerical schemes derived from each formulation will then be proposed. The equivalence between both numerical schemes will be proven under specific assumptions.

Continuum formulation

Lagrangian conservation law

The conservation law in Lagrangian coordinates was first introduced by Courant and Friedrich (1948) in the case of gas dynamics. In traffic flow, equation (1) becomes:

$$\partial_t s + \partial_n v = 0 \tag{3}$$

where the spacing s corresponds to $1/k$. The corresponding fundamental diagram V^* can be expressed as a concave function of s, $v=V^*(s)=V(1/s)$. Therefore, the LWR model in Lagrangian coordinates corresponds to the following hyperbolic equation in s:

$$\partial_t s + \partial_n V^*(s) = 0 \tag{4}$$

Wagner (1987) has proven the equivalence between (4) and (1) for weak solutions, even in vacuum cases where s is not defined; i.e., when $k=0$.

Lagrangian variational principle

The reader should refer to (Daganzo, 2005; 2005b) for a complete description of this theory in Eulerian coordinates. For simplicity, we will study here homogeneous problems but inhomogeneous ones can be treated similarly as in (Daganzo, 2005). Special inhomogeneous problems will be exemplified in section 4.

What follows shows that the transformation to Lagrangian coordinates preserves the nature of the problem; i.e. that a partial differential equation similar to (2) has to be solved:

$$\partial_t X = V^*\left(-\partial_n X\right) \tag{5}$$

derived from $v = V(1/k) = V^*(s)$. To prove the existence of $\partial_t X$ and $\partial_n X$, we only need to show that X exists and is differentiable. To this end, we note that the function $X(n,t)$ can be obtained by inverting $N(x,t)$; i.e., solving for x in $n=N(x,t)$. Two cases may arise:

(a) non-vacuum ($k=\partial_x N\neq 0$): in this case, N is continuous and strictly decreasing in space. Hence, $N(x,t)$ is bijective and the inversion is possible. Thus, $X(n,t)$ exists, is continuous and strictly increasing in n. Furthermore, as N is differentiable except on shockwaves, X verifies the same property.

(b) vaccum ($\partial_x N=0$ and $\partial_n X=+\infty$): this case corresponds to step-jumps in the X-profile with respect to n; i.e., voids in traffic flow. Intuitively, these jumps should not be a problem because a void separates two independent LWR problems: the solution of one does not influence the solution of the other. Reassuringly, Wagner's results (1987) imply that the general problem remains well-posed even when N is not invertible.

Therefore, it is possible to formulate the Lagrangian variational principle analogously to the Eulerian one; i.e., it can be treated similarly as in (Daganzo, 2005). One just has to transpose variables using Table 1.

	Eulerian coordinates	**Lagrangian coordinates**
Unknown function	N	X
Main variable	$k=-\partial_x N$	$s=-\partial_n X$
Flux	$q=\partial_t N$	$v=\partial_t X$
FD	$Q(k)$	$V^*(s)$

Table 1: Correspondence between the Eulerian and Lagrangian variational principles

All the results proven in (Daganzo, 2005 ; 2005b) can thus be applied to the Lagrangian variational formulation of the LWR model. Notably, the value of X at a point P in the (n,t) plane, X_P, can be expressed as a least-cost path problem:

$$X_P = \min\left(B_{\mathcal{P}} + \Delta\left(\mathcal{P}\right) : \forall \mathcal{P} \in \mathbf{V} \cap \mathbf{P}_P\right), \text{ where}$$

$$\begin{array}{l} \mathbf{V}\text{: set of all valid paths} \\ \mathbf{P}_P\text{: set of all path from the boundary condition to } P \\ B_{\mathcal{P}}: X \text{ value at the beginning of the path} \\ \Delta\left(\mathcal{P}\right)\text{: cost of path } \mathcal{P} \end{array} \tag{6}$$

Analogously to (Daganzo, 2005), "waves" in (n,t) coordinates are characteristics where s is constant, they have slopes $u=\partial_s V^*(s)$ representing a passing rate. We define two types of passing rates: (a) u is a "possible passing rate" if there exists s such that $u=\partial_s V^*(s)$; (b) $\hat{u}$ is an "allowable passing rate" if $\min(\partial_s V^*(s)) \leq \hat{u} \leq \max(\partial_s V^*(s))$. "Valid paths" are continuous and piecewise differentiable paths $n(t)$ in the (n,t) plane whose slopes $n'(t)$ are allowable passing rates. "Wave paths" are valid paths whose slopes are possible passing rates and are thus composed of a succession of waves.

The cost rate r on a wave path is given by $\mathrm{d}_t X$. The scalar r represents the speed of the Eulerian characteristic associated to the passing rate u.

$$r = \mathrm{d}_t X = \partial_t X + \partial_n X \partial_t n = v - su \tag{7}$$

As (5) holds and V^* is concave, one can express r only as a function $R(u)$ using the Legendre transformation as in (Daganzo, 2005):

$$r = R(u) = \sup_s \left\{ V^*(s) - su \right\} \tag{8}$$

The cost on a Lagrangian valid path $\mathcal{P}$ from B to P is thus:

$$\Delta(\mathcal{P}) = \int_{t_B}^{t_P} R\left(n'(t)\right) dt \tag{9}$$

In the next section, we will show how the Lagrangian variational principle makes it possible to construct a numerical scheme which is exact under few restrictive assumptions.

Numerical resolution

Godunov scheme

In the Godunov scheme, the spacing s is approximated by a constant value, s_i^t, between n and $n+\Delta n$ and is calculated every time step Δt; see Figure 1. Since the flux function V^* for equation (4) is non-decreasing in s, the characteristic speed is always non-negative (traffic anisotropy). The Godunov method reduces in this case to the upwind method:

$$s_i^{t+\Delta t} = s_i^t + \frac{\Delta t}{\Delta n}\left(V^*\left(s_i^t\right) - V^*\left(s_{i-1}^t\right) \right) \tag{10}$$

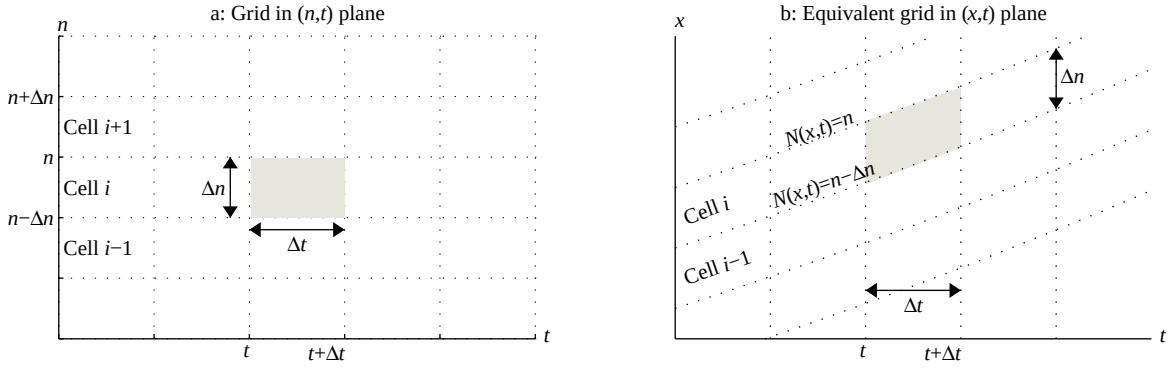

Figure 1: Lagrangian grid

The Courant-Friedrich-Lewy's (CFL) condition (11) defines the stability domain of (10). As the Godunov scheme is consistent and conservative, this also guarantees that it converges (Leveque, 1992).

$$\Delta n \geq \max_s \left| \partial_s \left(V^*(s) \right) \right| \Delta t \tag{11}$$

Notice that non-negative wave speeds imply that Lagrangian rarefaction waves never influence flux values at cell boundaries. The entropy condition is therefore naturally handled in the numerical scheme; i.e., it is not necessary to explicitly include the entropy condition in the numerical solution method.

The Lagrangian Godunov scheme can also be expressed in terms of $X(n,t)$ by noting that the flux $V^*(s_i^t)$ at a boundary n of a cell i is:

$$\frac{X(n,t+\Delta t)-X(n,t)}{\Delta t}=V^*(s_i^t)=V^*\left(-\frac{X(n,t)-X(n-\Delta n,t)}{\Delta n}\right) \tag{12}$$

If we suppose now that Q is triangular as in Figure 2a, V^* can be expressed as:

$$V^*(s)=\min\left(v_m, w\left(k_m s-1\right)\right) \tag{13}$$

where v_m is the free-flow speed, w, the wave speed and k_m, the jam density; see Figure 2b. After simplification (12) becomes:

$$X(n,t+\Delta t)=\min\left(X(n,t)+v_m\Delta t,(1-\alpha)X(n,t)+\alpha X(n-\Delta n,t)-w\Delta t\right) \tag{14}$$

where $\alpha=wk_m\Delta t/\Delta n$. If the CFL condition (11) is satisfied as an equality, then $\Delta n=wk_m\Delta t$ and $\alpha=1$. In this case, equation (14) reduces to:

$$X(n,t+\Delta t)=\min\left(X(n,t)+v_m\Delta t, X(n-\Delta n,t)-w\Delta t\right) \tag{15}$$

When n is an integer and $\Delta n=1$ then $X(n,t)$ corresponds to the position x_n^t of vehicle n at time t and $X(n\text{-}1,t)$ to the position x_{n-1}^t of its leader at the time t. Notice that equation (15) reduces to Newell's simplified car-following model (Newell, 2002) (Daganzo, 2006):

$$x_n^{t+\Delta t}=\min\left(x_n^t+\frac{v_m}{wk_m}, x_{n-1}^t-\frac{1}{k_m}\right) \tag{16}$$

We will show that this scheme is exact using the Lagrangian variational principle.

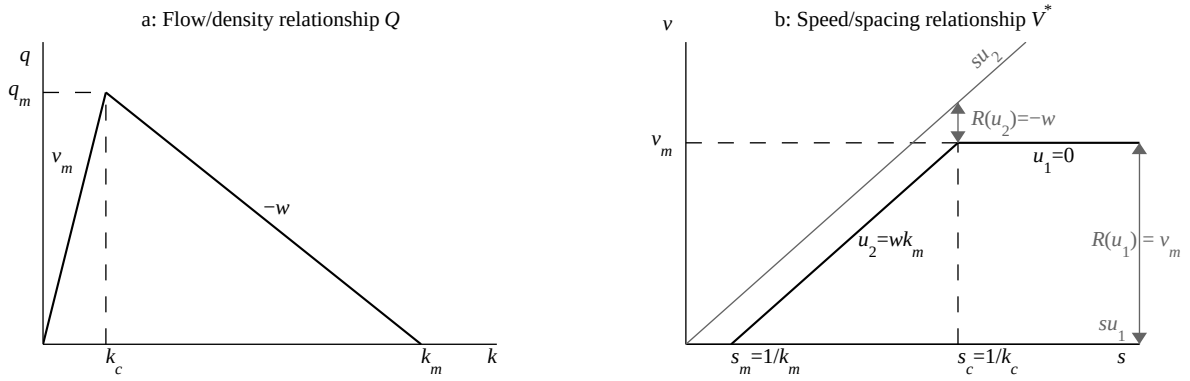

Figure 2: Triangular fundamental diagram

Lagrangian variational principle

Daganzo (2005b) proposed efficient methods to solve the LWR model using the concept of "sufficient networks". A "network" is defined as a directed graph of nodes and arcs in the

relevant plane (Eulerian or Lagrangian), where arcs are valid paths. A network is "sufficient" when the least-cost path through the network between every valid pair of nodes is an optimum path. A pair of nodes is said to be "valid" if a valid path exists between them. Notice that this valid path may not necessarily be included in the network. An "optimum path" between a valid pair of nodes is a least-cost valid path between these two points. Notice, again, that this optimum path may not be included in the network and this may introduce errors. In a sufficient network, the solution is exact at every node provided that the initial data is linear between two consecutive initial nodes.

Next, we will apply this method in Lagrangian coordinates to the variational principle (5) supposing that Q is triangular. In this case, waves have only two possible velocities: u_1=0 (free-flow) and u_2=wk_m (congestion). The resulting cost rates (8) are: $R(u_1)$=v_m and $R(u_2)$=-w; see Figure 2b. It can be shown, following the derivation in (Daganzo, 2005b), that any geometric network formed by two families of parallel equidistant lines with slopes u_1 and u_2 and separated by Δn_1 and Δn_2 is sufficient; see Figure 3a. Therefore, with appropriate initial data, the solution at nodes is exact.

Since u_1=0 nodes are always lined-up along rows where n values are constant. Furthermore, if one sets Δn_1=Δn_2=Δn nodes also line-up along "time-columns"; see Figure 3b. This defines a rectangular lattice in the (n,t) plane with Δt=$\Delta n/wk_m$, which is very practical for computational implementation. Furthermore, with only two incoming arcs per node, the computation of (6) at each node is straightforward; i.e.:

$$\begin{aligned} X(n,t+\Delta t) &= \min\left(X(n,t)+\Delta_{(n,t)\to(n,t+\Delta t)}, X(n-\Delta n,t)+\Delta_{(n-\Delta n,t)\to(n,t+\Delta t)}\right) \\ &= \min\left(X(n,t)+v_m\Delta t, X(n-\Delta n,t)-w\Delta t\right) \end{aligned} \tag{17}$$

where $\Delta_{(n,t)\to(n',t')}$ is the cost of the arc between the two grid-points (n,t) and (n',t').

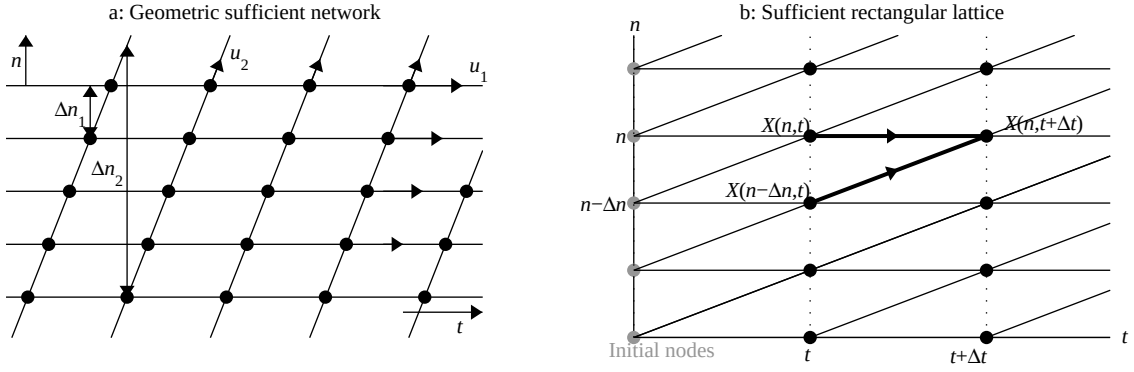

Figure 3: Geometric networks associated to the Lagrangian variational principle

Notice that (17) and (15) are identical. Therefore, the Godunov and the variational schemes are equivalent when Q is triangular and the CFL condition (11) is satisfied as an equality; i.e., when Δn=$wk_m\Delta t$. In this case, the Godunov scheme computes the exact solution and no numerical viscosity appears. This will be illustrated in the next section.

3. NUMERICAL ERRORS OF THE GODUNOV SCHEME IN EULERIAN COORDINATES

This section expresses the Godunov scheme in terms of the *N*-function in order to obtain insights about the nature of the numerical viscosity introduced by this scheme in Eulerian coordinates. This manipulation will allow us to quantify a bound for the global error. These results enhance the interest of the Lagrangian approach, which induces no numerical errors. Note that Q is supposed triangular in this section.

The Godunov scheme in Eulerian coordinates

In (x,t) coordinates, a highway is partitioned into small sections of length Δx and time into time-steps of duration Δt. The density of cell i at time t is approximated by a constant value, k_i^t. The Godunov scheme expresses the exit flow $q_i^{t\to t+\Delta t}$ of cell i between time t and $t+\Delta t$ as:

$$q_i^{t\to t+\Delta t} = \min\left(\lambda\left(k_i^t\right), \mu\left(k_{i+1}^t\right)\right) \tag{18}$$

where λ and μ correspond to the demand and supply functions; i.e.:

$$\lambda(k) = \min\left(v_m k, q_m\right) \quad \text{and} \quad \mu(k) = \min\left(w(k_m - k), q_m\right) \tag{19}$$

where q_m is the capacity. This scheme requires the CFL condition to be satisfied:

$$\Delta x \geq v_m \Delta t \tag{20}$$

The density $k_i^{t+\Delta t}$ is updated as usual considering the vehicle conservation law:

$$k_i^{t+\Delta t} = k_i^{t+\Delta t} + \frac{\Delta t}{\Delta x}\left(q_{i-1}^{t\to t+\Delta t} - q_i^{t\to t+\Delta t}\right) \tag{21}$$

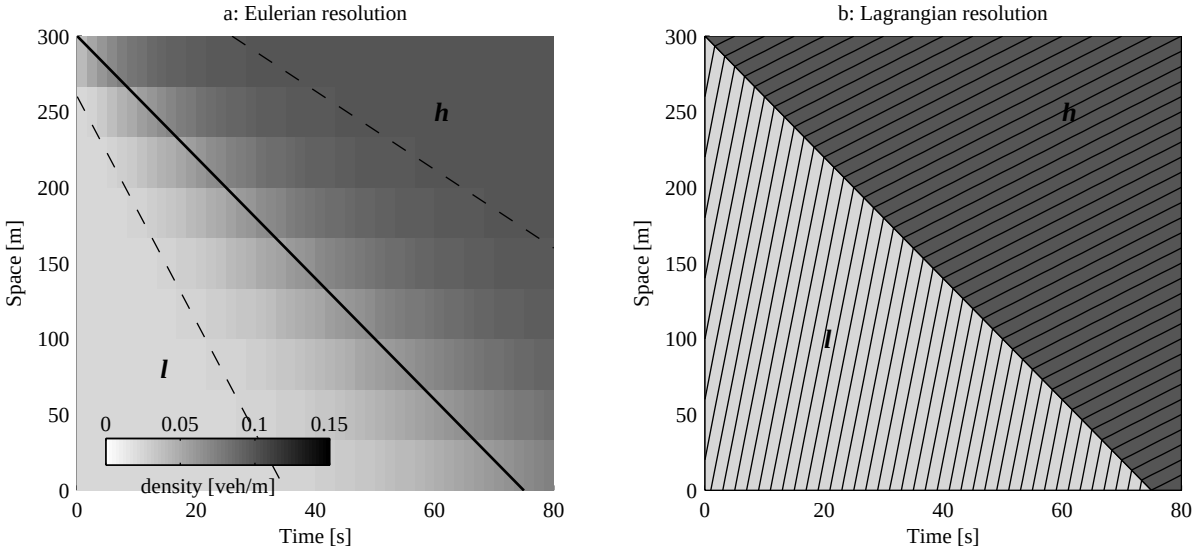

Figure 4: Comparison of the Eulerian and Lagrangian Godunov schemes

It is well known that this scheme induces numerical viscosity especially for shockwave propagating backwards a transition between a low density *l* and a higher density *h*. Viscosity

appears even if the shockwaves speed w_s is equal to $-w$ and the CFL condition is satisfied as an equality. This is illustrated in Figure 4a where we used v_m=20 m/s; w=4 m/s; k_m=0.15 veh/m; l=0.025 veh/m; h=0.1 veh/m; w_s=-4 m/s; Δt=1.67 s and Δx=33.3 m. Figure 4b shows the same experiment (using Δn=1) solved with the Lagrangian Godunov scheme of section 2, which is exact.

Notice in Figure 4a that the shockwave (shown as a solid slanted line) is increasingly smoothed out as time evolves; dotted lines have been added in the figure to indicate how the time-space region where errors occur grows in time. The exactness of the Lagrangian Godunov scheme is apparent from Figure 4b, as trajectories—represented by solid lines—change speeds precisely on the shockwave; shades of gray have been added to the figure to distinguish both traffic regimes.

Nature of the errors

Even though local truncation errors have been extensively analyzed in the mathematical literature (Leveque, 1992), no analytical expressions for the global errors have been published. The global error is defined here in L_∞ metric for all x and all t. To quantify this error, let us reformulate (18) in terms of $N(x,t)$ using $k=-\partial_x N$ and $q=\partial_t N$:

$$\frac{N(x,t+\Delta t)-N(x,t)}{\Delta t}=\min\left(\lambda\left(-\frac{N(x,t)-N(x-\Delta x,t)}{\Delta x}\right),\mu\left(-\frac{N(x+\Delta x,t)-N(x,t)}{\Delta x}\right)\right) \quad (22)$$

Combining (19) and (22) gives the variational form of the Godunov scheme:

$$N(x,t+\Delta t)=\min\left(N_A,N_B+wk_m\Delta t,N_C+q_m\Delta t\right) \text{ where} \quad (23)$$

$$\begin{cases} N_A=(1-\beta')N(x,t)+\beta' N(x-\Delta x,t) \\ N_B=(1-\beta)N(x,t)+\beta N(x+\Delta x,t) \\ N_C=N(x,t) \\ \beta=w\Delta t/\Delta x \text{ and } \beta'=v_m\Delta t/\Delta x \end{cases} \quad (24)$$

Note that $N(x, t+\Delta t)$ is calculated as the minimum between three wave paths[1], coming from the points A, B and C; see Figure 5a. Their slopes are respectively v_m, $-w$ and 0, and their Eulerian cost rates are 0, wk_m and q_m. The N-values at these points are N_A, N_B and N_C, respectively.

It is clear from Figure 5a that the Godunov scheme is exact only if N_A and N_B are known exactly. However, this is not true in general as A and B are generally not grid-points. Actually, as can be seen from (24), the N-value at these points is a weighted average of the N-values at the endpoints of their associated cell; see Figure 5b. Notice that N_A is known exactly when the CFL condition (20) is satisfied as an equality: i.e., $\Delta x=v_m\Delta t$. This implies that β'=1 and A is the grid-point $(x-\Delta x,t)$. However, N_B is known exactly only when Q is an isosceles triangle. In this case, $w=v_m$, β=1 and B is the grid-point $(x+\Delta x,t)$.

[1] Notice that horizontal paths are not wave paths in general but when Q is triangular they are optimum paths. Thus, they may be considered as wave paths here.

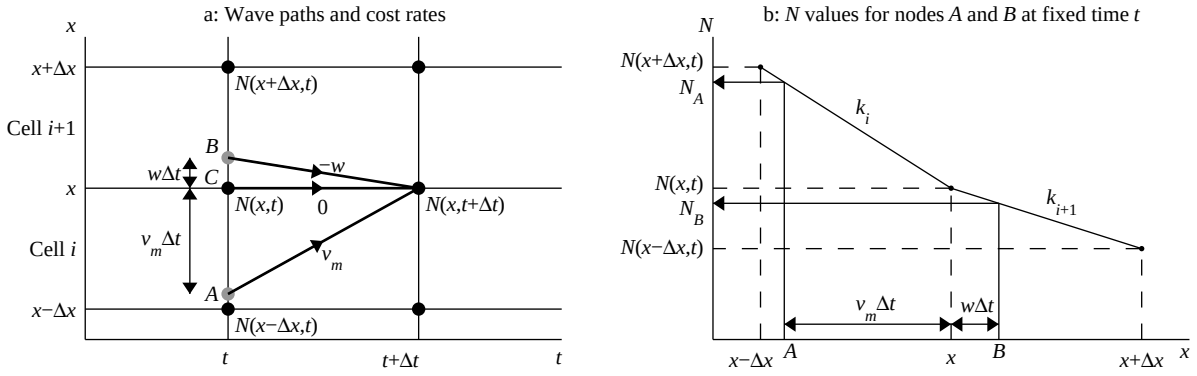

Figure 5: Formulation of the Eulerian Godunov scheme under a variational form

With the exception of isosceles FDs – which are not realistic –, numerical errors always arise when N_B is the minimum in (23). This happens for shockwaves propagating backwards. Shockwaves propagating forwards do not induce numerical errors when the CFL condition (20) is satisfied as an equality because N_A or N_C are the minimums in (23).

Quantification of the errors

We will now estimate analytically the numerical errors induced by the Godunov scheme, which is possible using equation (23). Let us consider two consecutives cells i and i+1 with densities l and h as shown in Figure 6a. A shockwave appears at time t_0 at the boundary x_1 between these two cells and propagates backwards at a velocity $-w$. For simplicity, we suppose that $\Delta x=v_m\Delta t$ and that the ratio $j=v_m/w$ is an integer[2]. Thus, the shockwave crosses the upstream boundary x_0 of cell i at time t_j after j time-steps; see Figure 6b. At time t_p ($1\leq p \leq j$), the numerical error, e_p, at x_0 between the numerical solution, $\tilde{N}$, and the exact one, N, is given by:

$$e_p = \tilde{N}\left(x_0, t_p\right) - N\left(x_0, t_p\right) \tag{25}$$

In this case, N_B is the minimum in (23). Thus, e_p can be expressed as:

$$\begin{aligned} e_p &= \tilde{N}\left(x_0 + w\Delta t, t_{p-1}\right) - N\left(x_0 + w\Delta t, t_{p-1}\right) \\ &= \tilde{N}\left(x_1, t_{p-1}\right) + l_{p-1}\left(\Delta x - w\Delta t\right) - \left[N\left(x_1, t_{p-1}\right) + \left(p-1\right)hw\Delta t + \left(\Delta x - pw\Delta t\right)l\right] \end{aligned} \tag{26}$$

where $l_{p\text{-}1}$ represents the estimated density in cell i at time $t_{p\text{-}1}$. Note that $\tilde{N}(x_1, t_{p-1})$ and $N(x_1, t_{p-1})$ are identical because the flow calculated by the Godunov scheme at the boundary x_1 is always equal to q_h, which is the exact solution. It follows that e_p becomes:

$$e_p = \Delta x\left(1-\alpha\right)\left(l_{p-1} - l\right) - \alpha\left(p-1\right)\Delta x\left(h-l\right) \tag{27}$$

where $\alpha=w\Delta t/\Delta x=w/v_m$.

At time t_p, the estimated density l_p can be expressed by the following recursion:

$$l_p = \left(1-\alpha\right)l_{p-1} + \alpha h = \left(1-\left(1-\alpha\right)^p\right)h + \left(1-\alpha\right)^p l \tag{28}$$

[2] if it is not the case, it can be shown that the global error computed in this subsection is an upper bound.

By replacing $l_{p\text{-}1}$ in (27), e_p becomes:

$$e_p = \left[-(1-\alpha)^p - \alpha p + 1\right](h-l)\Delta x \tag{29}$$

Finally, as $j=1/\alpha$, e_j is given by:

$$e_j = (1-\alpha)^{1/\alpha}(l-h)\Delta x \tag{30}$$

As expected, the error is proportional to Δx and to the density difference l-h. Interestingly, the error is also decreasing in α, which means that the more the congested branch of the FD is flat the more the errors are important. Notice that the error contribution of α can be bound by exp(-1); i.e. $|e_j| \leq 0.37|l\text{-}h|\Delta x$. Actually, this bound is rather tight for typical values of α ($4 \leq 1/\alpha \leq 8$). Notice too, that e_j is an upper bound for the global error (i.e., for all $t \geq t_j$ and all $x \leq x_0$) since the Godunov scheme is a contraction mapping and e_j represents the maximum error at x_0 for all t.

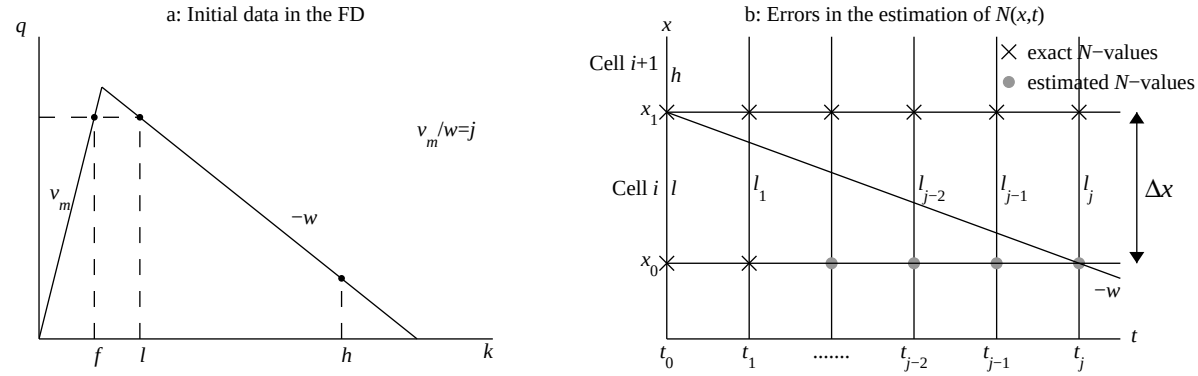

Figure 6: Global error induced by the Godunov scheme for shockwave propagation backwards

Finally, in the more general case of a shockwave, where the upstream density corresponds to a free-flow traffic state (e.g., f in Figure 6a), it can be shown that (30) represents an upper-bound to the global error provided that l corresponds to the congested density associated to the flow $v_m f$; see Figure 6a.

4. EXTENSIONS USING THE LAGRANGIAN VARIATIONAL PRINCIPLE

This section examines how to incorporate existing extensions to the LWR model into the Lagrangian variational principle. In this section, we will suppose that Q is triangular and that $\Delta n=1$.

Moving bottlenecks

In analogy with the Eulerian case, exogenous moving bottlenecks (see Newell, 1998, Lebacque et *al*, 1998; and Leclercq et *al*, 2004 for a review) can be represented as moving boundary conditions. Thus, they represent shortcuts in the solution network (Daganzo and

Menedez, 2005). As described in section 2, the cost rate of each arc of the shortcut becomes the speed of the bottleneck, v_b, while the slope of the arc in (n,t) is the bottleneck's passing rate, r_b; see Figure 7a.

The only caveat is that in multilane/single-pipe highways r_b is not know a priori and therefore the arc cannot be introduced in advance. Note that in single-lane highways (or multilane/multi-pipe) this problem does not exist since r_b is always equal to 0. In fact, this problem only arises in multilane/single-pipe highways when the moving bottleneck is not active. In this case r_b depends on traffic conditions, i.e. $r_b=q-kv_b$; when it is active r_b is set to its maximum value, $\hat{r}_b$.

A general numerical solution method including moving bottlenecks may be described as follows between times t and $t+\Delta t$:

(i) include the shortcut arc (arc a_s in Figure 7b) assuming $r_b = \hat{r}_b$; let B_j be the point of intersections of the shortcut and the network. Notice that this point may intersect either arc a_1 with slope $u_1=0$ (case a in Figure 7b) or arc a_2 with slope $u_2=wk_m$ (case b in Figure 7b).

(ii) calculate the value of X at the point B_j by applying (6) to the two possible paths: $B_{j-1}\rightarrow B_j$ and $(n,t)\rightarrow B_j$ (case a) or $(n-1,t)\rightarrow B_j$ (case b).

(iii) if the optimum path to B_j does not include the shortcut arc then set r_b such that the value of X at B_j is the same on both paths; this condition ensures that r_b is consistent with traffic conditions and that the bottleneck is not active.

(iv) calculate the value of X at the grid-point $(n,t+\Delta t)$ by applying (6) to the two possible paths: $B_j\rightarrow(n,t+\Delta t)$ and $(n-1,t)\rightarrow(n,t+\Delta t)$ (case a) or $(n,t)\rightarrow(n,t+\Delta t)$ (case b).

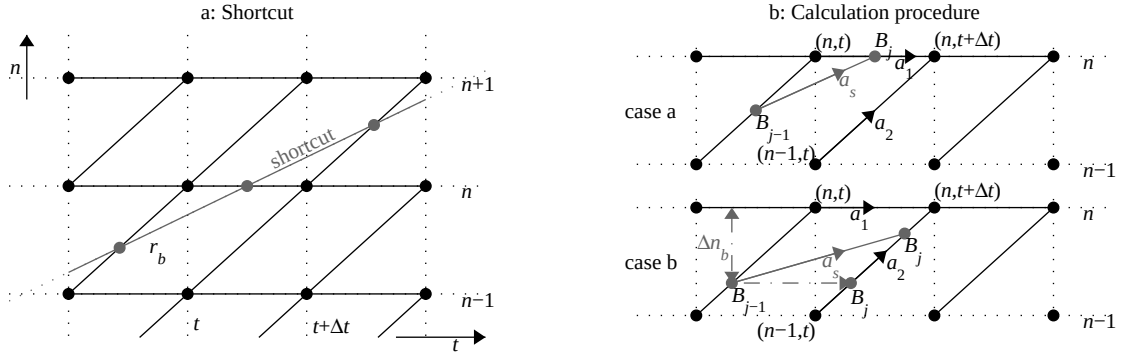

Figure 7: Moving bottlenecks

In the case of a single-lane, the above numerical method simplifies significantly. Only case b in Figure 7b can take place with a horizontal bottleneck trajectory as shown by the dotted line in the figure. Notice that the bottleneck is introduced at a "distance" Δn_b from its leader; this distance is determined when the bottleneck is first introduced, and is constant thereafter.

It can be shown that the position of the bottleneck and its follower are given by:

$$\begin{aligned} X_{B_j} &= \min(X_{B_{j-1}} + v_b \Delta t, X\left(n-1,t\right) - \frac{\Delta n_b}{k_m}) \quad \text{(bottleneck)} \\ X\left(n,t+\Delta t\right) &= \min(X(n,t) + v_m \Delta t, X_{B_j} - \frac{1-\Delta n_b}{k_m}) \quad \text{(follower)} \end{aligned} \tag{31}$$

Finally, it is worth to note that fixed bottlenecks can be treated in the same way described above by setting v_b=0 and noting that passing rates correspond to the flow crossing the bottleneck. Again, except in cases where r_b can be determined exogenously (e.g., a traffic signal in red phase) the general procedure described above must be utilized.

Self-similar highways

A self-similar highway is composed of successive segments whose FDs are scaled versions of each other; e.g., a highway where the number of lanes varies in space. This means that the set of wave speeds is the same on all segments and that maximum passing rates are multiples of each other. Unfortunately, as opposed to Eulerian coordinates, this problem is harder to treat in Lagrangian coordinates because:

(a) the Lagrangian trajectory of boundaries between segments is not known a priori (for the same reasons than for bottlenecks).
(b) maximum passing rates are different on each segment, which makes it hard to define the network for the whole highway.
(c) if the ratio between different FDs is not a rational number, a sufficient network does not exist and therefore exact solutions can not be found.

Intersections

Existing intersection models split the supply (available capacity) of an outgoing link considering demands on incoming links (see Lebacque and Koshyaran, 2005 for a review). Different models differ in the way they treat demands, but the inputs are the same. Therefore, in the Lagrangian variational principle all one needs to do is computing supplies and demands. This can be accomplished using (19) and properly defining the densities. To this end, we use the method in (Leclercq, 2006) where supplies and demands are computed whenever a vehicle crosses the intersection boundary. It can be shown that in this case the density for computing demands is the inverse of the upstream spacing; the density for computing supplies is the inverse of the downstream spacing. Next, one only has to apply the desired intersection model and incorporate the resulting flow allocation as a fixed boundary condition in space. This boundary corresponds to a bottleneck at the downstream end of each incoming link, and to initial data at the entry of each outgoing link.
The method remains exact as long as the numerical grid-points of every link coincide; i.e., when the FD is the same on all links. Otherwise, one would need to interpolate between grid-

points and this would introduce numerical errors that will propagate, and which may or may not grow when passing through neighbouring intersections.

Vehicle characteristics

The Lagrangian framework is the natural environment for introducing vehicle characteristics since it is a coordinate system that "moves" with the flow. Furthermore, if we consider (as in this subsection) a single lane, then $X(n,t)$ represents the trajectory of vehicle n since $\Delta n=1$. In this case, the inclusion of vehicle-specific characteristics becomes straightforward. For example, information such as origin and destination (O/D), vehicle number or drivers' value of time are trivial to incorporate because it does not modify the network (and thus the car-following rule). However, for incorporating characteristics such as maximum desired speed, vehicle acceleration capabilities or driver-specific FDs one must modify the network. Some examples are given next.

Different free-flow speeds

If drivers have different free-flow speeds one may simply change the cost rate of the horizontal arcs of the solution network to the free-flow speed of the particular driver. This is illustrated in Figure 8a, where v_m^n is the desired free-flow speed of vehicle n. Notice that this implementation is straightforward because the network geometry remains unchanged. Only the costs are modified.

Different reaction times

If drivers have different reactions times, they will exhibit different values of w. In this case, the network geometry changes because the slope of the slanted arcs between two consecutive vehicles varies. This is illustrated in Figure 8b where w_n is the wave speed of vehicle n. The time-step implementation of this extension is not straightforward as grid-points are no longer aligned on a regular lattice as shown the by the dotted lines in the figure. It is possible that event programming or approximating w_n by rational numbers may streamline the solution method.

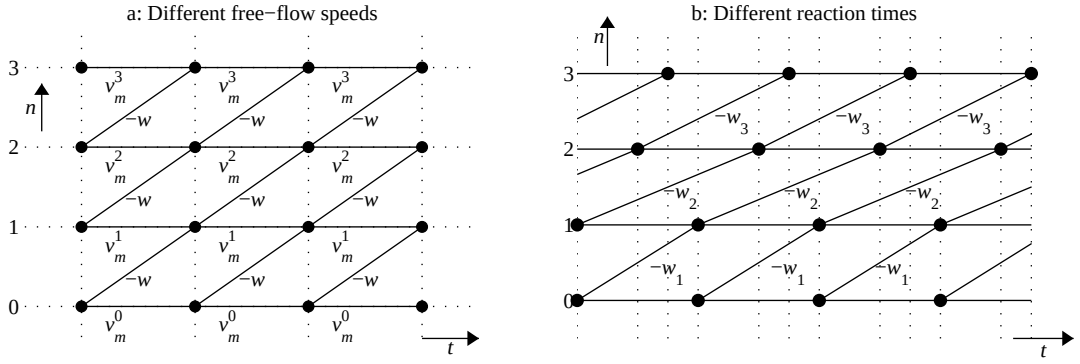

Figure 8: Examples of network for incorporating vehicle characteristics

Bounded vehicle acceleration

In the literature (Lebacque, 2003, Leclercq, 2006) this extension has been conceived for obtaining realistic acceleration profiles when transitioning to a less congested traffic state, as opposed to the infinite accelerations produced by the LWR model.
In Lagrangian coordinates, this can be accomplished similarly as in the case of different free-flow speeds presented above. The only difference is that $v_m^n = v_m^n(t)$; i.e.,

$$v_m^n(t+\Delta t) = v_m^n(t) + a(t)\Delta t \tag{32}$$

were $a(t)$ is the desired acceleration of vehicle n at time t which may depend on vehicle type, roadway geometry, current speed, etc.

Multi-pipe solution method

We refer to a multi-pipe approach when each freeway lane is considered as an independent unit that interacts with adjacent lanes via lane changes. In this case, the solution method for including bottlenecks simplifies significantly compared to multilane/single-pipe highways. This happens because in a single lane bottleneck passing rates are zero, and so are shortcut arc slopes. This implies that one may construct the solution network beforehand without having to modify it due to varying passing rates.
Furthermore, bottlenecks can be used to represent the blockage effect of lane-changing vehicles on the target lane as in Laval and Daganzo (2006). The only complication is the incorporation of forced lane-changing manoeuvres when drivers accept very short non-equilibrium gaps and force their way into the target lane. This phenomenon—commonly observed in the field—can be incorporated using the framework proposed in this paper via the relaxation procedure proposed in Laval and Leclercq (2006). This procedure allows drivers to accept short gaps while gradually attaining safer equilibrium ones.

5. DISCUSSION

From the authors' point of view, the main advantage of the Lagrangian approach is its exactness when Q is triangular. This is important because a triangular Q is parsimonious while being an accurate representation of reality. Although exactness for triangular FDs is shared by the Eulerian variational numerical methods, further extensions are much easier to incorporate in Lagrangian coordinates provided that a multi-pipe approach is used. This is illustrated in Table 2, which shows the easiness of implementation for the extensions discussed in section 4. Notice that in Lagrangian coordinates, there is only one column because the Godunov and the variational schemes are equivalent when Q is triangular; see section 2. The double entries in the table highlight that a multilane/single-pipe representation makes it difficult to incorporate some extensions in Lagrangian coordinates. Again, this is not the case in the multi-pipe representation because passing rates are known a priori.

	Lagrangian approach	**Eulerian approach**	
Extensions	**Godunov/variational schemes**	**Godunov scheme**	**Variational method**
Moving bottlenecks	++ (multi-pipe) -- (multilane / single-pipe)	+ (Daganzo and Laval, 2005a) - (Daganzo and Laval, 2005b)	++
Fixed bottlenecks	++ (multi-pipe) -- (multilane / single-pipe)	++ (Lebacque, 1996)	++
Self-similar highways	++ (multi-pipe) -- (multilane / single-pipe)	++ (Lebacque, 1996)	++
Vehicle characteristics (same FD)	++	- for O/D (Daganzo, 1995)	?
Vehicle characteristics (modified FD)	++ (multi-pipe) ? (multilane / single-pipe)	- for bounded acceleration (Leclercq, 2006); ? otherwise	?
Lane-changing	-	- (Laval and Daganzo, 2006)	?
Intersections	+	+ (Lebacque et Koshyaran, 2005)	+

Table 2: Extension implementation complexity by approach
(++: very easy; + easy; - not so easy; -- difficult; ? not known as yet)

Table 3 presents a summary of the exactness of the different approaches analysed in this paper. At a glance, the superiority of the Lagrangian approach is apparent as it remains exact in all cases but the Godunov scheme when Q is piecewise linear with more than two wave speeds (PWL). The nature of the error in this case is similar to the Eulerian Godunov case in section 3; i.e., X needs to be interpolated between grid points. We note that when Q is PWL the Eulerian variational numerical method introduces errors because one is forced to introduce horizontal arcs (see Daganzo, 2005b, §3.1) which are not necessarily wave paths. Interestingly, in the Lagrangian counterpart, horizontal arcs are also needed but correspond to wave paths. Therefore, no numerical errors are introduced. Another interesting advantage of the Lagrangian variational method is that it does not require $v_m/w=j$ to be an integer in order to have a rectangular lattice; in the Eulerian counterpart, this is not only necessary but one has to memorize for the j time-steps preceding the current simulation time.

	Lagrangian approach		**Eulerian approach**	
	Godunov scheme	**Variational method**	**Godunov scheme**	**Variational method**
***Q* triangular + rectangular lattice**	√	√	×	√ only if v_m/w is an integer and memory is used
***Q* triangular**	√	√	×	√ only for geometric networks
***Q* PWL**	×	√	×	×

Table 3: Exactness by approach (√:exact; ×: non exact)

With respect to the computational cost for the Godunov scheme, consideration of (15) and (18) reveals that a Lagrangian cell imposes approximately a third of the elementary operations imposed by an Eulerian cell. For the variational approach, the number of elementary

operations is roughly equivalent in Lagrangian and in Eulerian coordinates. To have an idea, let us define congestion as a mean density higher than $(k_c+k_m)/2$. For a given Δt, the Lagrangian approach is more efficient than the Eulerian variational method as long as less 30% of the network is congested; it is always more efficient than the Eulerian Godunov method under this definition of congestion.
Finally, further research is needed to ensure that when coupling together different extensions in Lagrangian coordinates no compatibility problems arise. For example, provided that different reaction times imply uneven time-steps, conflicts may arise with bottlenecks or intersections models. The use of memory in Lagrangian networks may provide a solution for such compatibility problems.

6. ACKNOWLEDGMENT

The authors would like to thank Professor Carlos Daganzo for suggesting the use of variational theory in Lagrangian coordinates. This work has been partially supported by the French ACI-NIM (Nouvelles Interactions des Mathématiques) N°193 (2004).

7. REFERENCES

Courant, R. and Friedrichs, K.O. (1948). Supersonic Flows and Shock Waves. *Pure Appl. Math*, **1**.

Daganzo, C.F. (2006). In traffic flow, cellular automata = kinematic waves. *Transportation Research B*, **40**(5), 396-403.

Daganzo, C.F. (2005). A variational formulation of kinematic waves: basic theory and complex boundary conditions. *Transportation Research B*, **39**(2), 187-196.

Daganzo, C.F. (2005b). A variational formulation of kinematic waves: Solution methods. *Transportation Research B*, **39**(10), 934-950.

Daganzo, C.F. (1995). The cell transmission model, part II: network traffic. *Transportation Research B*, **29**(2), 79-93.

Daganzo, C.F. (1994). The cell transmission model: A dynamic representation of highway traffic consistent with the hydrodynamic theory. *Transportation Research B*, **28**(4), 269-287.

Daganzo, C.F. and Laval, J.A. (2005). On the numerical treatment of moving bottlenecks. *Transportation Research B*, **39**(1), 31-46.

Daganzo, C.F. and Laval, J.A. (2005b). Moving bottlenecks: A numerical method that converges in flows. *Transportation Research B*, **39**(9), 855-863.

Daganzo, C.F. and Menendez, M. (2005). A variational formulation of kinematic waves: bottlenecks properties and examples. In: Mahmassani H.S. (Ed.), *16th ISTTT*, Pergamon, London, 345-364.

Godunov, S.K. (1959). A difference scheme for numerical computation of discontinuous solutions of equations of fluid dynamics. *Mat. Sb.* **47**, 271-290.

Laval, J.A., Daganzo, C.F. (2006). Lane-changing in traffic streams. *Transportation Research B*, **40**(3), 251-264.

Lebacque, J.P. (2003). Two-phase bounded-acceleration traffic flow model: analytical solutions and applications. *Transportation Research Record*, **1852**, 220-230.

Lebacque, J.P. (1996). The Godunov scheme and what it means for first order traffic flow models. In: Lesort J.B. (Ed.), *13th ISTTT*, Pergamon, London, 647-678.

Lebacque, J.P., Koshyaran, M.M. (2005). First order macroscopic traffic flow models: intersections modeling, network modeling. In: Mahmassani, H.S. (Ed.), *16th ISTTT*, Pergamon, London, 365-386.

Lebacque, J.P., Lesort, J.B., Giorgi, F. (1998). Introducing buses into first-order macroscopic traffic flow models. *Transportation Research Record*, **1644**, 70-79.

Leclercq, L. (2006). Hybrid resolution of the LWR model. *85th Transportation Research Board Annual Meeting* [CDROM]. Washington: Transportation Research Board, 16p. *Submitted for publication*.

Leclercq, L. (2006). Bounded acceleration close to fixed and moving bottlenecks. *Transportation Research B*, accepted for publication.

Leclercq, L., Chanut, S., Lesort, J.B., (2004). Moving bottlenecks in the LWR model: a unified theory. *Transportation Research Record*, **1883**, 3-13.

Leveque, R.J. (1992). Numerical methods for conservation laws. *2nd Edition*. Bâle: Switzerland, Birkhäuser, 214 p.

Lighthill, M.J. and Whitham, J.B. (1955). On kinematic waves II: A theory of traffic flow in long crowded roads. *Proceedings of the Royal Society*, **A229**, 317-345.

Newell, G.F. (2002). A simplified car-following theory: a low-order model. *Transportation Research B*, **36**(3), 195-205.

Newell, G.F. (1998). A moving bottleneck. *Transportation Research B*. **32**(8), 531-537.

Newell, G.F. (1993). A simplified theory of kinematic waves in highway traffic, part I General Theory. *Transportation Research B,* **27**(4), 281-287.

Richards, P.I. (1956). Shockwaves on the highway. *Operations Research*, **4**, 42-51.

Wagner, D. (1987). Equivalence of the Euler and Lagrangian equations of gas dynamics for weak solutions. *J. Diff. Eq*., **68**, 118-136.